Workshop

Numerical Modeling of Earthquake Motions: Waves and Ruptures

July 5-9, 2015
Smolenice Castle near Bratislava, Slovakia

Numerical Study of Site Effects in a Class of Local Sedimentary Structures

Jozef **Kristek** Peter **Moczo**
Pierre-Yves **Bard** Fabrice **Hollender**
Svetlana **Stripajová** Zuzana **Margočová**

Comenius University in Bratislava

ISTerre : Institute of Earth Science, Grenoble, France

CEA : Commissariat à l'énergie atomique, Cadarache, France

Earth Science Institute, Slovak Academy of Sciences, Bratislava

we have spent some time

to develop our

FD and FD-FE

numerical-modeling methodology

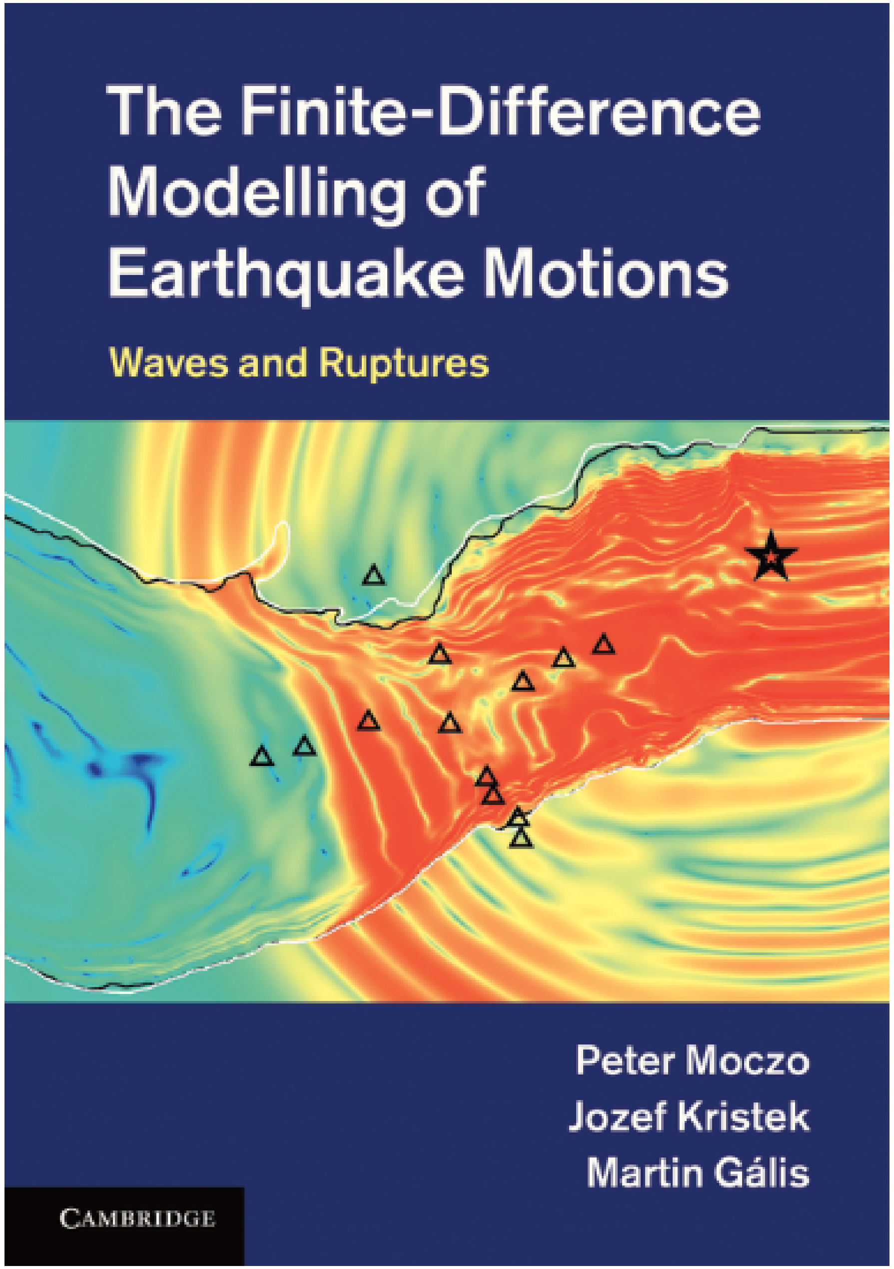

recently

we have got an opportunity

to become useful

depth of the sediment-basement interface
in the Mygdonian basin (Site 1)

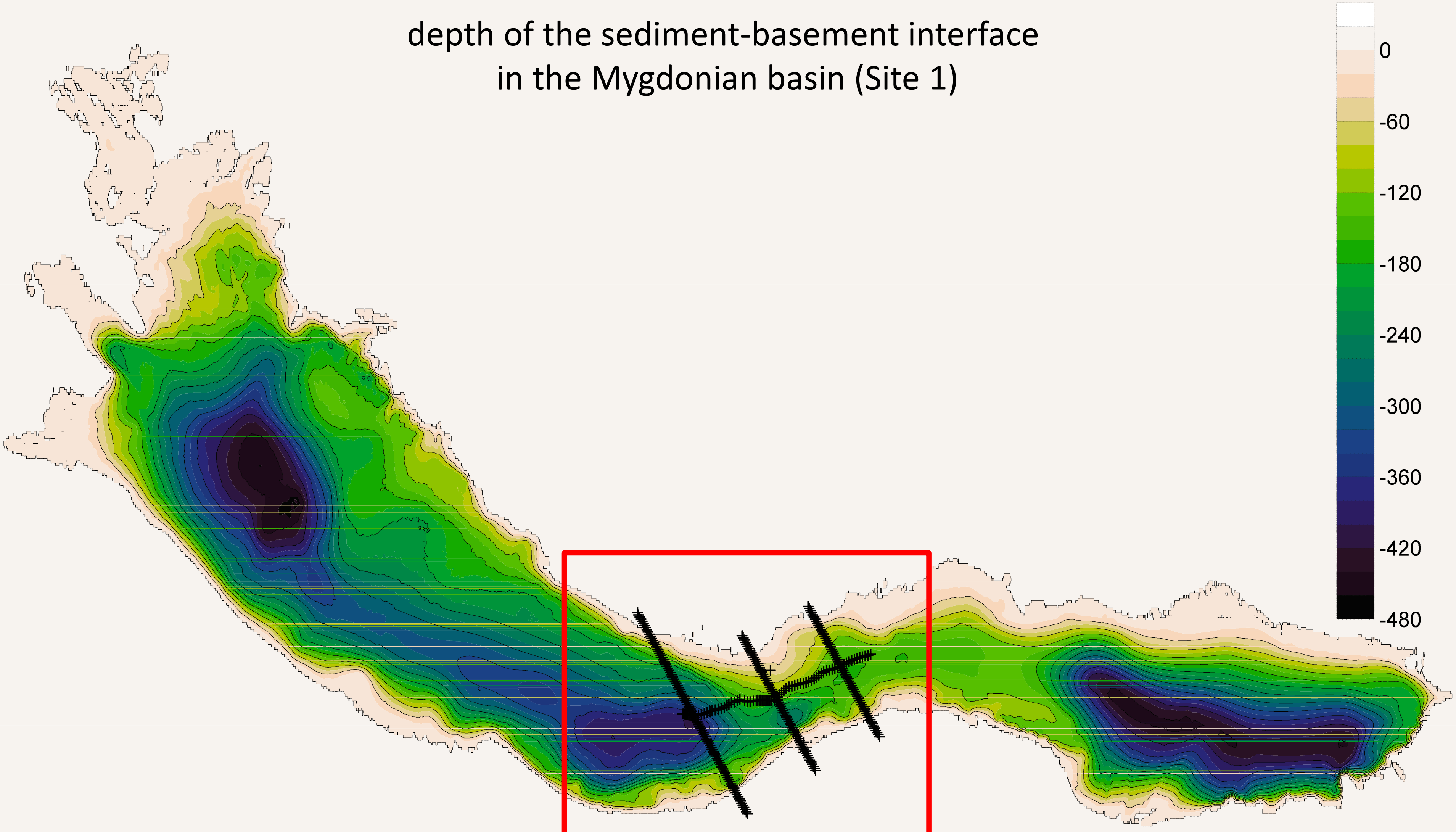

depth of the sediment-basement interface in the Grenoble valley (Site 2)

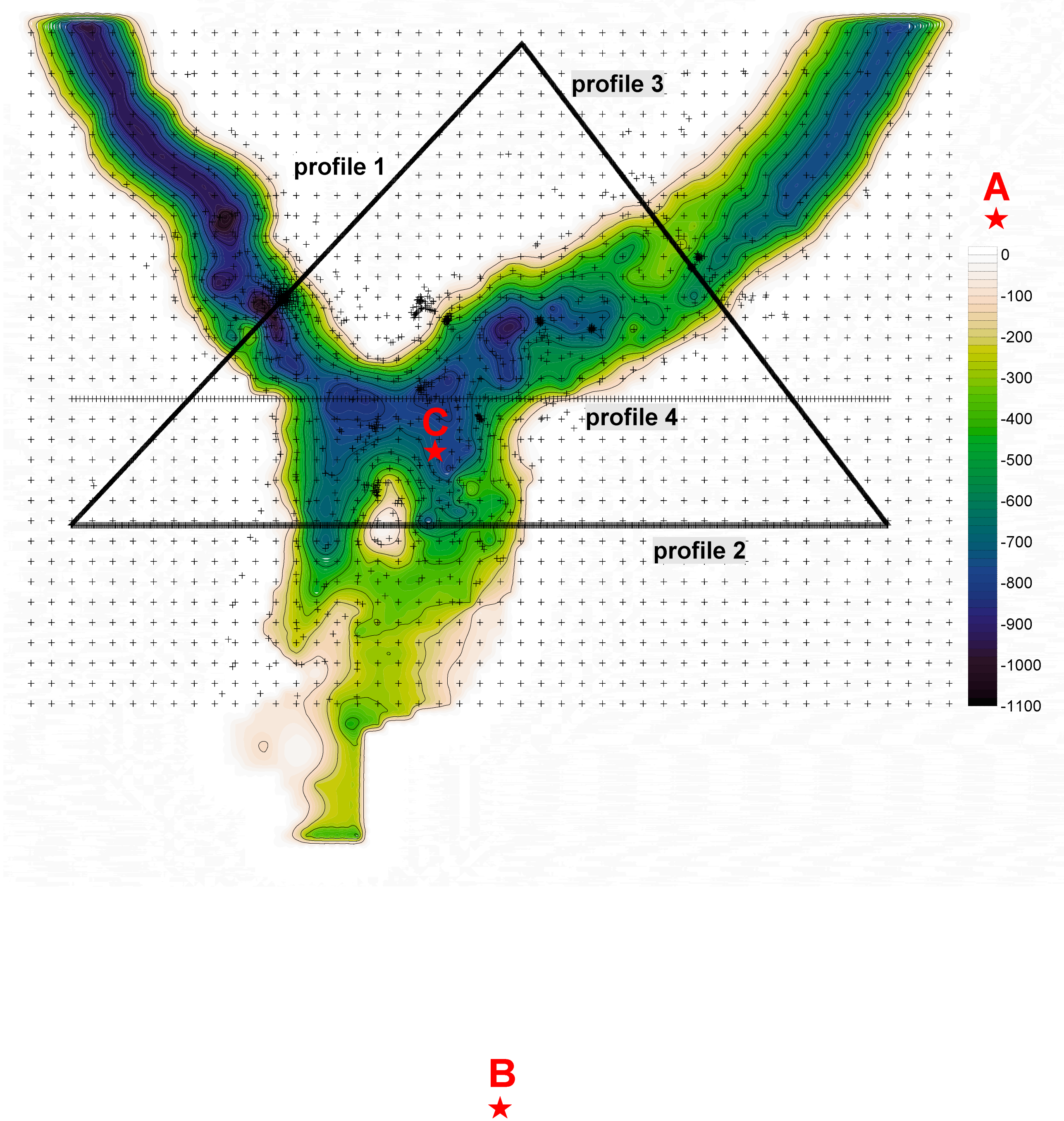

geometry of the sediment-basement interface in the nominal-model profiles

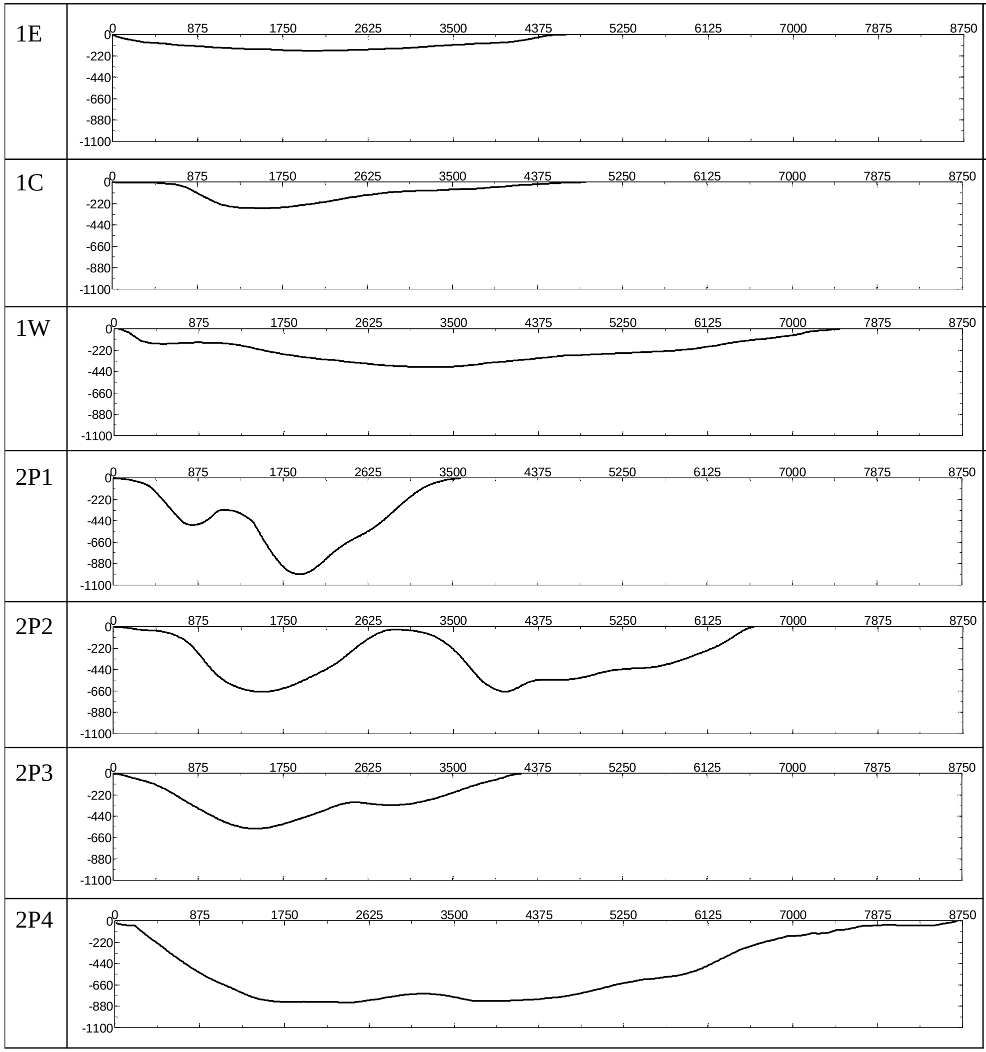

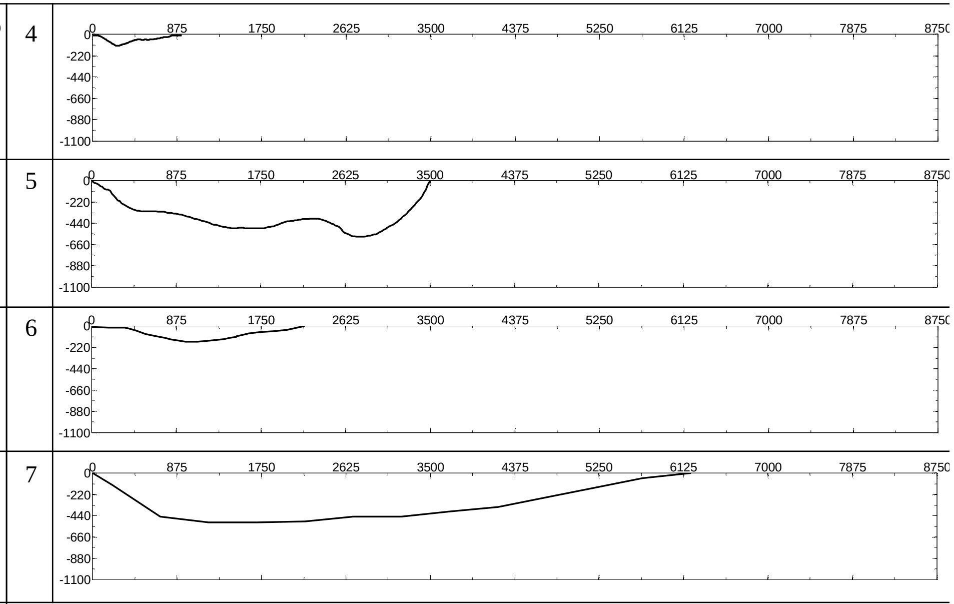

all profiles are absolutely scaled

S-wave speed distribution in the nominal-model profiles

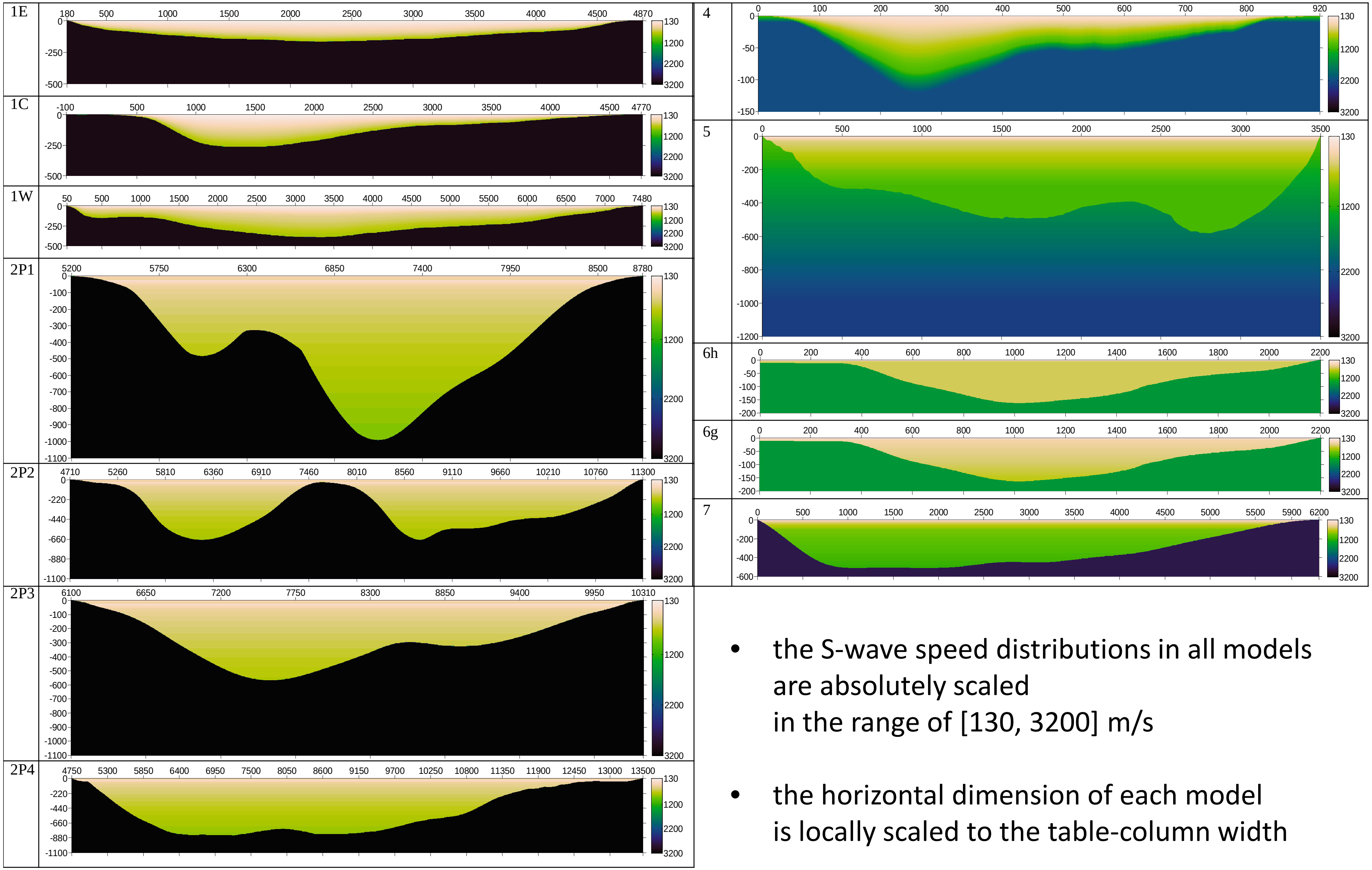

- the S-wave speed distributions in all models are absolutely scaled
  in the range of [130, 3200] m/s
- the horizontal dimension of each model
  is locally scaled to the table-column width

sites and models – table of parameters

Site		$V_{S_{30}}$	$\overline{V}_S$	W	z_{max}	$V_{S_{bedrock}}$	f_{00}	z_{max}/W	$V_{S_{bedrock}}/V_{S_{30}}$
		$[m/s]$	$[m/s]$	$[m]$	$[m]$	$[m/s]$	$[1/s]$	$[1]$	$[1]$
Site1 (Mygdonian basin)	1E	180	400	4 700	167	2 600	0.7	0.04	14.5
	1C	170	445	4 900	266		0.5	0.05	15.4
	1W	175	520	7 450	393		0.5	0.05	15
Site2 (Grenoble valley)	2P1	380	680	3 580	993	3 200	0.2	0.3	8.5
	2P2		610	6 590	670		0.3	0.1	
	2P3		590	4 210	570		0.3	0.1	
	2P4		660	8 750	844		0.2	0.1	
Site4		400	700	920	120	2 200	2.2	0.2	5.5
Site5		410	920	3 500	581	2 363	0.5	0.2	5.7
Site6	6h	540	590	2 200	161	1 500	0.9	0.07	2.8
	6g	390	530						3.9
Site7		400	960	6 200	510	2 800	0.5	0.08	7

project SIGMA

Se**I**smic **G**round **M**otion **A**ssessment

EDF, CEA, Areva and ENEL

project SIGMA

Se**I**smic **G**round **M**otion **A**ssessment

EDF, CEA, Areva and ENEL

task for the
Comenius University Bratislava team
in collaboration with ISTerre and CEA

investigate a potential of the specified sites
to cause **site effects**
using 1D, 2D and 3D numerical simulations

identify **key structural parameters**
affecting earthquake ground motion

we performed

3D simulations for 3 3D local surface sedimentary structures,

2D simulations for 12 2D structures

(*some of them being selected 2D profiles in the 3D structures*),

and 1D simulations for local 1D models in the 2D models

assuming

a vertical plane-wave incidence for all specified local structures,

point DC sources for one 3D structure,

and linear behaviour

using

a set of selected reference accelerograms

we investigated

earthquake ground motion

in the set of the defined local sedimentary structures

and

effects of uncertainty

in the bedrock velocity,

velocity in sediments,

attenuation in sediments,

interface geometry (border slope),

simultaneous variations in velocity and thickness of sediments

on

10 characteristics of earthquake ground motion

two selected configurations

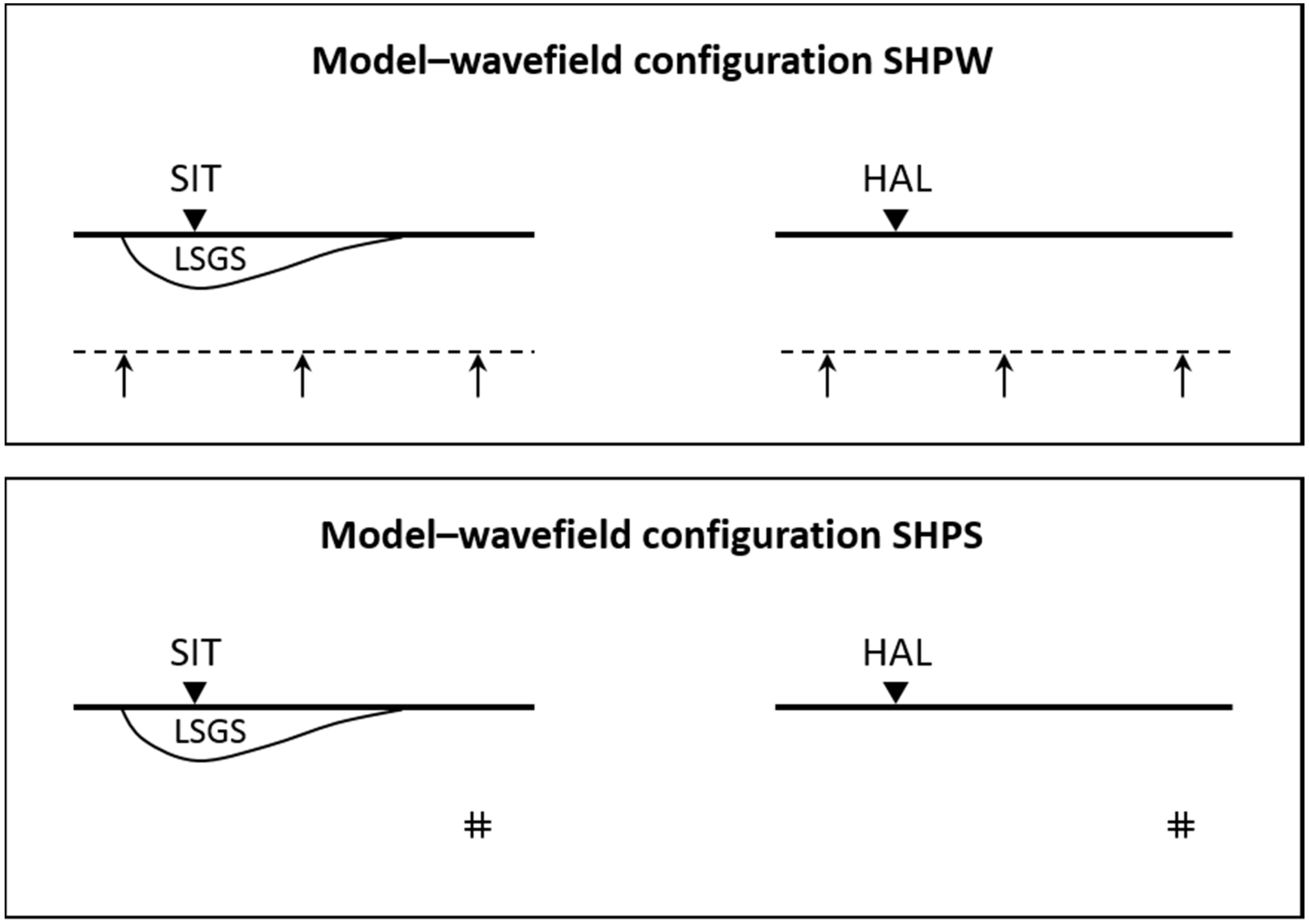

table of numerical simulations

Site	profile		Nominal model						Velocity in sediments						Attenuation in sediments									Border slope (BS)								Velocity in bedrock								Locally fixed fundamental frequency (modified velocity and thickness of sediments)				3D meander extension
									Modification of the nominal model																																			
									w/oHVL						NLQ			Elastic		VS/20		VS/40		BS/2_a		BS×2_a		BS/2_b		BS×2_b		1200		2000		3000		grad		- 40%		+ 40%		
		Dim	3				2	1	3				2	1	3	2	1	2	1	2	1	2	1	2	1	2	1	2	1	2	1	2	1	2	1	2	1	2	1	2	1	2	1	3
		Exc	DC			P	P	P	DC			P	P	P	P	P	P	P	P	P	P	P	P	P	P	P	P	P	P	P	P	P	P	P	P	P	P	P	P	P	P	P	P	P
			A	B	C				A	B	C																																	
S1	pE					*	*	*																																				
	pC					*	*	*																																				
	pW					*	*	*																																				
S2	p1		*	*	*	*	*	*	*	*	*	*	*	*	*	*	*							*	*	*	*																	
	p2		*	*	*	*	*	*	*	*	*	*	*	*	*	*	*																											
	p3		*	*	*	*	*	*	*	*	*	*	*	*	*	*	*																											
	p4		*	*	*	*	*	*	*	*	*	*	*	*	*	*	*																											
S4							*	*																																				
S5							*	*												*	*	*	*	*	*	*	*					*	*	*	*	*	*	*	*					
S6h							*	*										*	*	*	*	*	*	*	*	*	*	*	*	*	*	*	*	*	*	*	*	*	*	*	*	*	*	*
S6g							*	*										*	*	*	*	*	*	*	*	*	*	*	*	*	*	*	*	*	*	*	*	*	*					*
S7							*	*										*	*	*	*	*	*									*	*	*	*	*	*	*	*					

Legend:

Dim – dimension: **3** = 3D, **2** = 2D, **1** = 1D; **Exc** – excitation: **DC** = point double-couple source, **P** = plane wave

HVL = high-velocity layer; **NLQ** = Q derived from nonlinear simulation

$$\mathrm{P}* \sim \mathbf{R} \equiv \begin{bmatrix} r_{xx} & r_{yx} & r_{zx} \\ r_{xy} & r_{yy} & r_{zy} \\ r_{xz} & r_{yz} & r_{zz} \end{bmatrix}$$

$$\mathrm{DC}* \sim \quad \mathbf{S}_{elem}^{HAL} \equiv \begin{bmatrix} s_x^{1,HAL} & s_x^{2,HAL} & s_x^{3,HAL} & s_x^{4,HAL} & s_x^{5,HAL} & s_x^{6,HAL} \\ s_y^{1,HAL} & s_y^{2,HAL} & s_y^{3,HAL} & s_y^{4,HAL} & s_y^{5,HAL} & s_y^{6,HAL} \\ s_z^{1,HAL} & s_z^{2,HAL} & s_z^{3,HAL} & s_z^{4,HAL} & s_z^{5,HAL} & s_z^{6,HAL} \end{bmatrix}$$

$$\mathbf{S}_{elem}^{SIT} \equiv \begin{bmatrix} s_x^{1,SIT} & s_x^{2,SIT} & s_x^{3,SIT} & s_x^{4,SIT} & s_x^{5,SIT} & s_x^{6,SIT} \\ s_y^{1,SIT} & s_y^{2,SIT} & s_y^{3,SIT} & s_y^{4,SIT} & s_y^{5,SIT} & s_y^{6,SIT} \\ s_z^{1,SIT} & s_z^{2,SIT} & s_z^{3,SIT} & s_z^{4,SIT} & s_z^{5,SIT} & s_z^{6,SIT} \end{bmatrix}$$

frequency ranges for calculation of characteristics

<table>
<tr><th rowspan="2">site</th><th rowspan="2">profile</th><th colspan="3">dimension</th></tr>
<tr><th>3D</th><th>2D</th><th>1D</th></tr>
<tr><td rowspan="3">S1</td><td>pE</td><td rowspan="3">0.5 – 5 Hz</td><td colspan="2" rowspan="3">0.5 – 5 Hz
0 – 20 Hz</td></tr>
<tr><td>pC</td></tr>
<tr><td>pW</td></tr>
<tr><td rowspan="4">S2</td><td>p1</td><td rowspan="4">0.5 – 5 Hz</td><td colspan="2" rowspan="4">0.5 – 5 Hz
0 – 20 Hz</td></tr>
<tr><td>p2</td></tr>
<tr><td>p3</td></tr>
<tr><td>p4</td></tr>
<tr><td>S4</td><td></td><td></td><td colspan="2">0 – 20 Hz</td></tr>
<tr><td>S5</td><td></td><td></td><td colspan="2">0 – 20 Hz</td></tr>
<tr><td>S6h</td><td></td><td>0.5 – 7 Hz</td><td colspan="2">0.5 – 7 Hz
0 – 20 Hz</td></tr>
<tr><td>S6g</td><td></td><td>0.5 – 7 Hz</td><td colspan="2">0.5 – 7 Hz
0 – 20 Hz</td></tr>
<tr><td>S7</td><td></td><td></td><td colspan="2">0 – 20 Hz</td></tr>
</table>

key aspects
of a sufficiently
accurate and (<u>at the same time</u>) computationally efficient
algorithm based on a FD scheme

sufficiently

- realistic rheological model ~ GMB EK/GZB
- (optionally) low grid dispersion
  in a homogeneous medium for VP/VS up to ≈ 10 ~ (2,4) VS SG FDS
- accurate representation of the free-surface condition ~ AFDA
- accurate representation of the boundary condition
  at a material interface ~ volume orthorhombic averaging
- efficient grid ~ arbitrary spatial discontinuous grid
- accurate and efficient non-reflecting grid boundaries ~ PML

arbitrary-discontinuous
staggered grid

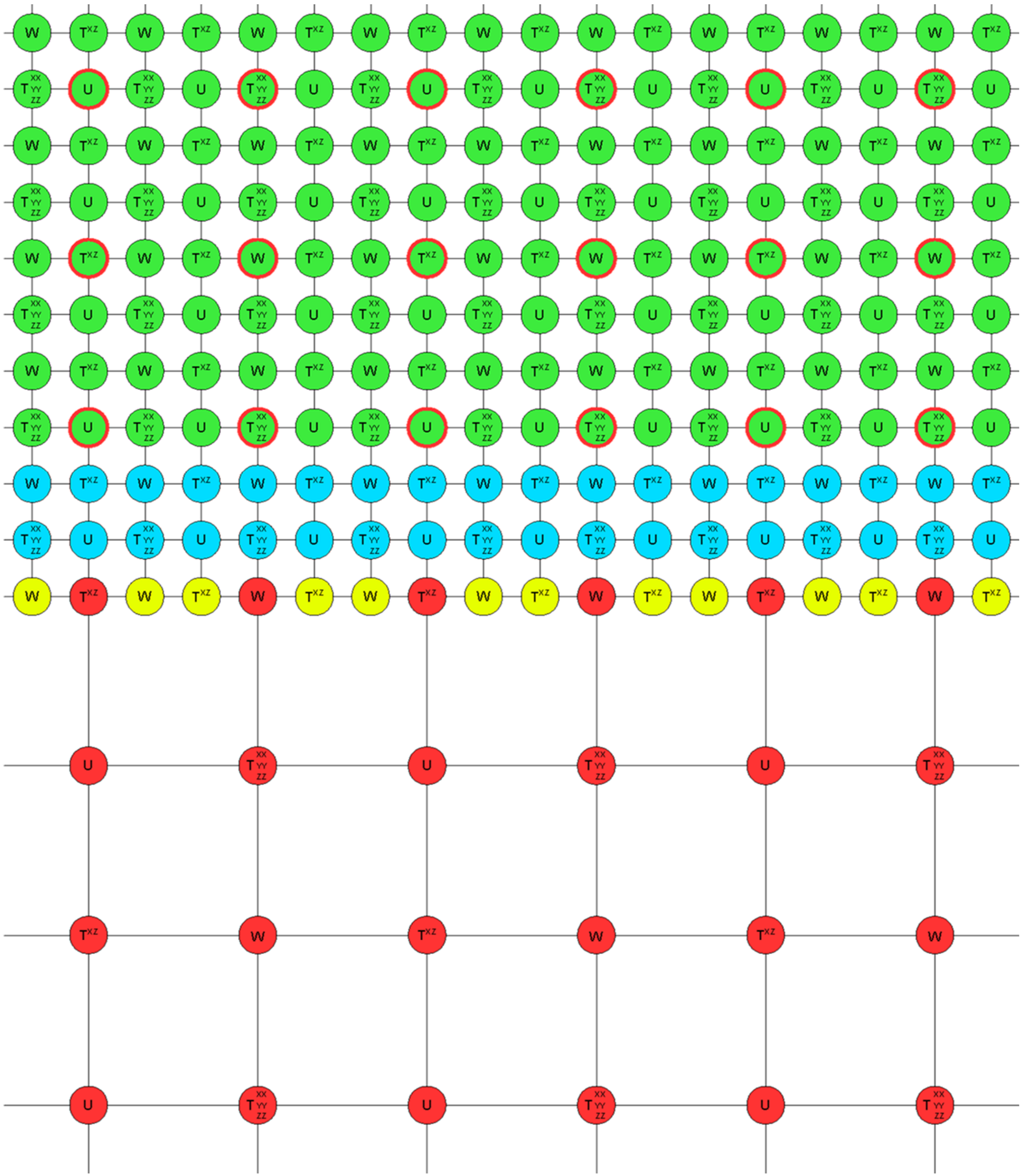

$$\frac{h_{\mathrm{COARSE}}}{h_{\mathrm{FINE}}} = \text{odd number}$$

we numerically tested
ratios **up to 25**

discontinuous grid: numerical example of efficiency

3D Grenoble valley modelling [0.5, 5] Hz

uniform grid:	8×10^9	grid points
discontinuous grid:	0.6×10^9	grid points
		that is
		7.5% of the uniform grid

$$\left\langle \sigma_{xy} \right\rangle^{z} = 2 \left\langle \left\langle \mu \right\rangle^{z} \right\rangle^{Hxy} \left\langle \varepsilon_{xy} \right\rangle^{xy}$$

$$\left\langle \sigma_{yz} \right\rangle^{x} = 2 \left\langle \left\langle \mu \right\rangle^{x} \right\rangle^{Hyz} \left\langle \varepsilon_{yz} \right\rangle^{yz}$$

$$\left\langle \sigma_{zx} \right\rangle^{y} = 2 \left\langle \left\langle \mu \right\rangle^{y} \right\rangle^{Hzx} \left\langle \varepsilon_{zx} \right\rangle^{zx}$$

$$\sigma_{xx} = \Pi_{x} \varepsilon_{xx} + \lambda_{xy} \varepsilon_{yy} + \lambda_{zx} \varepsilon_{zz}$$

$$\sigma_{yy} = \lambda_{xy} \varepsilon_{xx} + \Pi_{y} \varepsilon_{yy} + \lambda_{yz} \varepsilon_{zz}$$

$$\sigma_{zz} = \lambda_{zx} \varepsilon_{xx} + \lambda_{yz} \varepsilon_{yy} + \Pi_{z} \varepsilon_{zz}$$

the averaged medium

is

a medium with the **orthorhombic** anisotropy

with 9 independent coefficients

$$\Pi_x = \left\langle \left\langle M - \frac{\lambda^2}{M} \right\rangle^{yz} + \left[\left\langle \frac{\lambda}{M} \right\rangle^{yz} \right]^2 \langle M \rangle^{Hyz} \right\rangle^{Hx}$$

$$\Pi_y = \left\langle \left\langle M - \frac{\lambda^2}{M} \right\rangle^{zx} + \left[\left\langle \frac{\lambda}{M} \right\rangle^{zx} \right]^2 \langle M \rangle^{Hzx} \right\rangle^{Hy}$$

$$\Pi_z = \left\langle \left\langle M - \frac{\lambda^2}{M} \right\rangle^{xy} + \left[\left\langle \frac{\lambda}{M} \right\rangle^{xy} \right]^2 \langle M \rangle^{Hxy} \right\rangle^{Hz}$$

$$\lambda_{xy} = \left\langle \left\langle M - \frac{\lambda^2}{M} \right\rangle^z + \left[\left\langle \frac{\lambda}{M} \right\rangle^z \right]^2 \langle M \rangle^{Hz} \right\rangle^{Hxy} \left\langle \frac{\left\langle \lambda - \frac{\lambda^2}{M} \right\rangle^z + \left[\left\langle \frac{\lambda}{M} \right\rangle^z \right]^2 \langle M \rangle^{Hz}}{\left\langle M - \frac{\lambda^2}{M} \right\rangle^z + \left[\left\langle \frac{\lambda}{M} \right\rangle^z \right]^2 \langle M \rangle^{Hz}} \right\rangle^{xy}$$

$$\lambda_{yz} = \left\langle \left\langle M - \frac{\lambda^2}{M} \right\rangle^x + \left[\left\langle \frac{\lambda}{M} \right\rangle^x \right]^2 \langle M \rangle^{Hx} \right\rangle^{Hyz} \left\langle \frac{\left\langle \lambda - \frac{\lambda^2}{M} \right\rangle^x + \left[\left\langle \frac{\lambda}{M} \right\rangle^x \right]^2 \langle M \rangle^{Hx}}{\left\langle M - \frac{\lambda^2}{M} \right\rangle^x + \left[\left\langle \frac{\lambda}{M} \right\rangle^x \right]^2 \langle M \rangle^{Hx}} \right\rangle^{yz}$$

$$\lambda_{zx} = \left\langle \left\langle M - \frac{\lambda^2}{M} \right\rangle^y + \left[\left\langle \frac{\lambda}{M} \right\rangle^y \right]^2 \langle M \rangle^{Hy} \right\rangle^{Hzx} \left\langle \frac{\left\langle \lambda - \frac{\lambda^2}{M} \right\rangle^y + \left[\left\langle \frac{\lambda}{M} \right\rangle^y \right]^2 \langle M \rangle^{Hy}}{\left\langle M - \frac{\lambda^2}{M} \right\rangle^y + \left[\left\langle \frac{\lambda}{M} \right\rangle^y \right]^2 \langle M \rangle^{Hy}} \right\rangle^{zx}$$

computational aspects
–
time and memory

- 3D simulations: **60**
- 2D a 1D simulations: **305**
- total wall time: **220 days** (of errorless simulations)
- total CPU time: **37 years** assuming one CPU
- disk space for the synthetic seismograms and calculated EGM characteristics: **3 TB** (**TO**)

calculated EGM characteristics for each receiver position and each component

<table>
<tr><th colspan="2">Absolute EGM characteristic χ</th><th>Relative EGM characteristics</th><th>Average relative EGM characteristics</th><th>Averages</th><th>2D/1D, 3D/2D, 3D/1D aggravation factors</th></tr>
<tr><td>S_D</td><td rowspan="3">Calculated
for all receiver positions
for each pair
$[s_{\xi,i}(\mathrm{t}), a_{\xi,i}(\mathrm{t})]$
$i=1,\ldots,n$
$\xi \in \{x,y,z\}$</td><td rowspan="2">Amplification factor
$AF_{\xi,i}(\chi)$</td><td rowspan="2">Average (i) amplification factor
$\overline{AF_{\xi}}(\chi)$</td><td>short-period
long-period
f_0-centred
f_{00}-centred</td><td rowspan="3"></td></tr>
<tr><td>pga
pgv
CAV
I_A
a_{rms}
SI</td><td rowspan="2"></td></tr>
<tr><td>D_{TB}^{95}
D_{TB}^{75}</td><td>Prolongation factor
$PF_{\xi,i}(\chi)$</td><td>Average (i) prolongation factor
$\overline{PF_{\xi}}(\chi)$</td></tr>
<tr><td colspan="6">S_D - relative displacement response spectrum, pga - peak ground acceleration
pgv - peak ground velocity, CAV - cumulative absolute velocity, I_A - Arias intensity
a_{rms} - root-mean-square acceleration, SI - spectrum intensity
D_{TB}^{95} and D_{TB}^{75} - durations of strong ground motion</td></tr>
</table>

cumulative absolute velocity $$CAV\left(s_{\xi,i}(\vec{x})\right) \equiv \int_0^\infty \left| s_{\xi,i}(\vec{x},t) \right| dt$$

CAV amplification factor $$AF_{\xi,i}\{CAV\} \equiv \frac{CAV\left(s_{\xi,i}(\vec{x})\right)}{CAV\left(a_{\xi,i}(\vec{x})\right)}$$

average *CAV* amplification factor $$\overline{AF_{\xi}}\{CAV\} \equiv \sqrt[n]{\prod_{i=1}^{n} AF_{\xi,i}\{CAV\}}$$

CAV aggravation factor $$AGF_{\xi,32}(\varphi) \equiv \frac{\varphi_{\xi,\mathrm{3D}}}{\varphi_{\xi,\mathrm{2D}}}$$

peak ground acceleration

$$pga_{\xi,i}(\vec{x}) \equiv \max_t \left\{ \left| s_{\xi,i}(\vec{x},t) \right| \right\}$$

rms acceleration

$$a_{rms}\left(s_{\xi,i}(\vec{x})\right) \equiv \left[\frac{0.9}{t^{95}\left(s_{\xi,i}(\vec{x})\right) - t^{5}\left(s_{\xi,i}(\vec{x})\right)} \int_{t^{5}\left(s_{\xi,i}(\vec{x})\right)}^{t^{95}\left(s_{\xi,i}(\vec{x})\right)} s_{\xi,i}^{2}(\vec{x},t)\, dt \right]^{1/2}$$

$$t^{95}\left(s_{\xi,i}(\vec{x})\right) \equiv t\ \left(csa\left(t; s_{\xi,i}(\vec{x})\right) = 0.95\, mcsa\left(s_{\xi,i}(\vec{x})\right) \right)$$

$$t^{5}\left(s_{\xi,i}(\vec{x})\right) \equiv t\ \left(csa\left(t; s_{\xi,i}(\vec{x})\right) = 0.05\, mcsa\left(s_{\xi,i}(\vec{x})\right) \right)$$

$$mcsa\left(s_{\xi,i}(\vec{x})\right) \equiv \int_0^\infty s_{\xi,i}^{2}(\vec{x},t)\, dt$$

$$csa\left(t; s_{\xi,i}(\vec{x})\right) \equiv \int_0^t s_{\xi,i}^{2}(\vec{x},\tau)\, d\tau$$

set of
12 selected accelerograms

Mw:	4.6 - 6.5
epic. distance:	2 – 20 km
RJB distance:	1-16 km

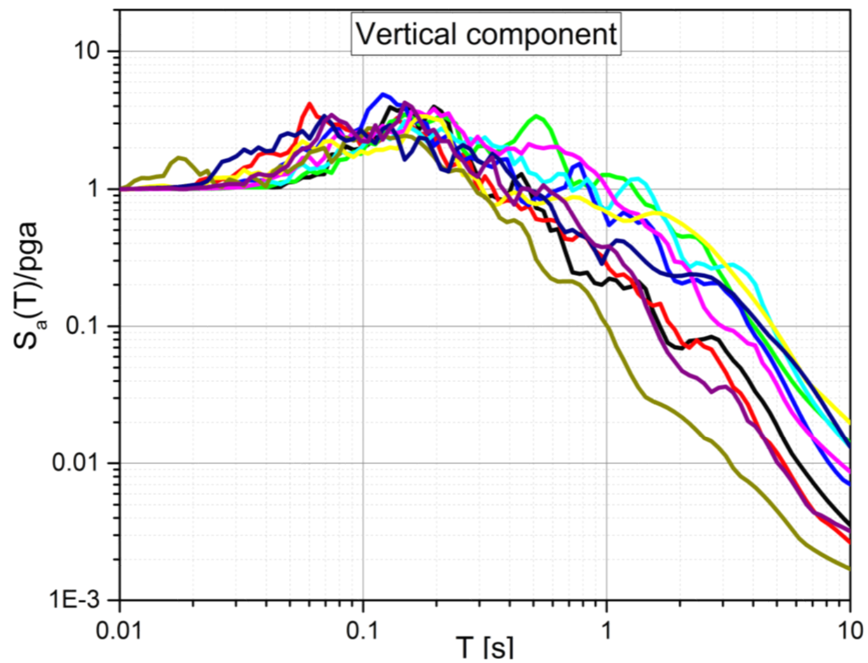

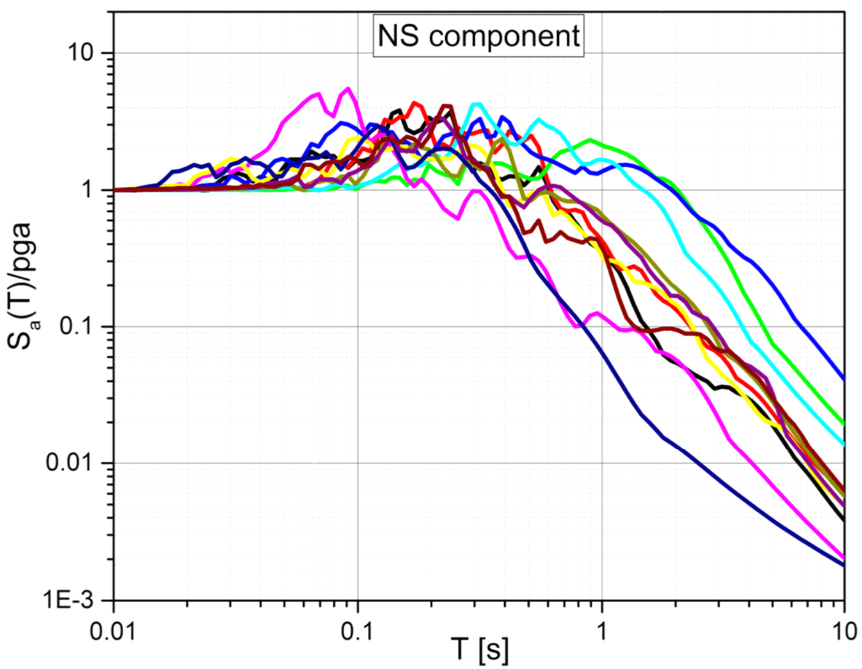

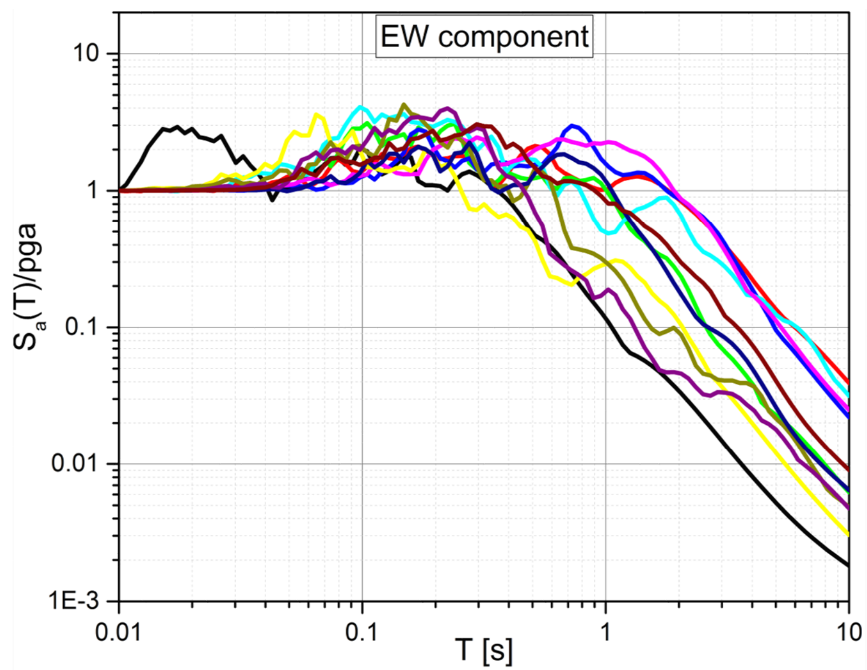

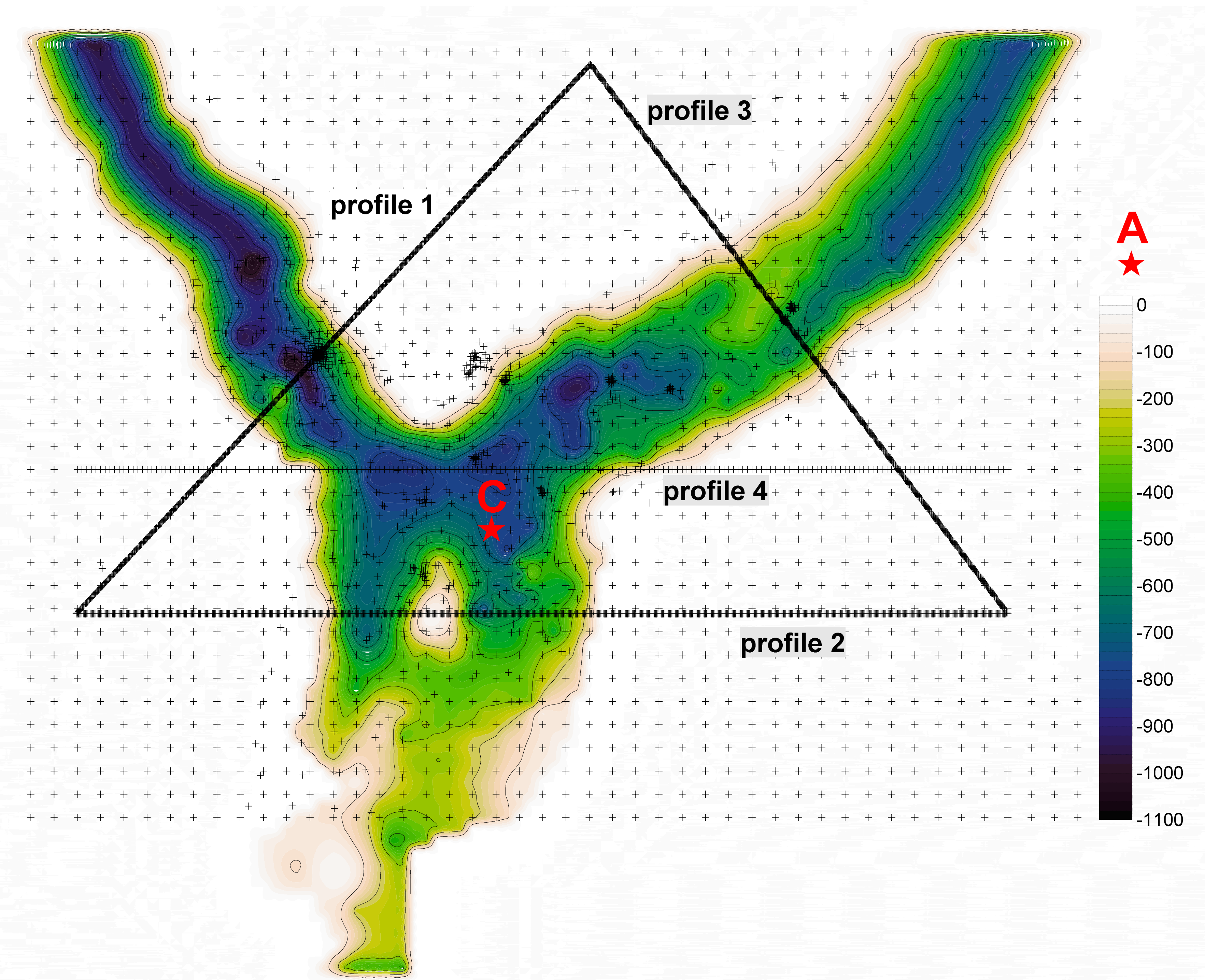
profile 1
profile 2
profile 3
profile 4
A
C
0
-100
-200
-300
-400
-500
-600
-700
-800
-900
-1000
-1100

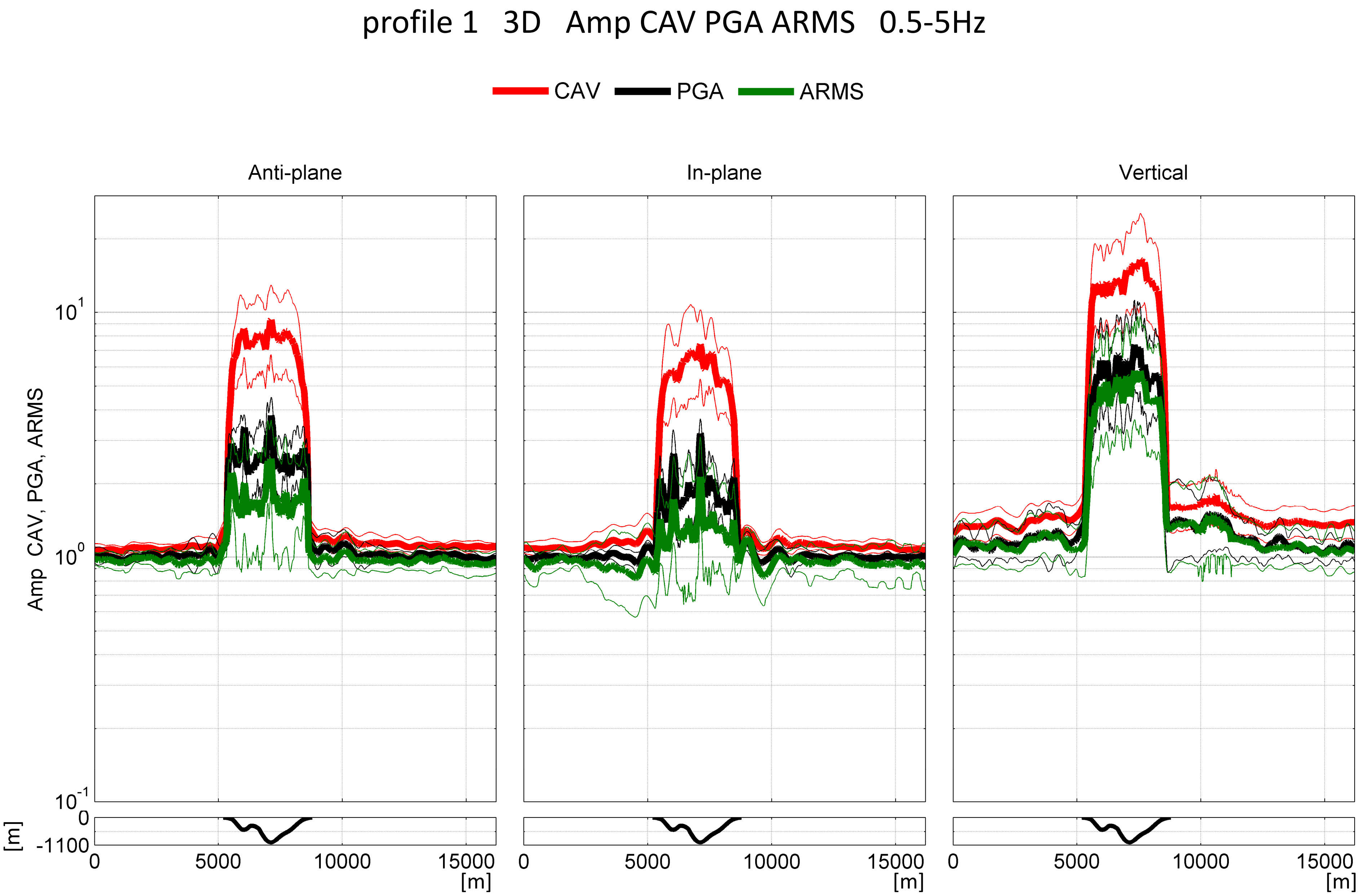

profile 1 3D Amp CAV PGA ARMS 0.5-5Hz
CAV
PGA
ARMS
Anti-plane
In-plane
Vertical
Amp CAV, PGA, ARMS
10^{1}
10^{0}
10^{-1}
[m]
0
-1100
0
5000
10000
15000
[m]

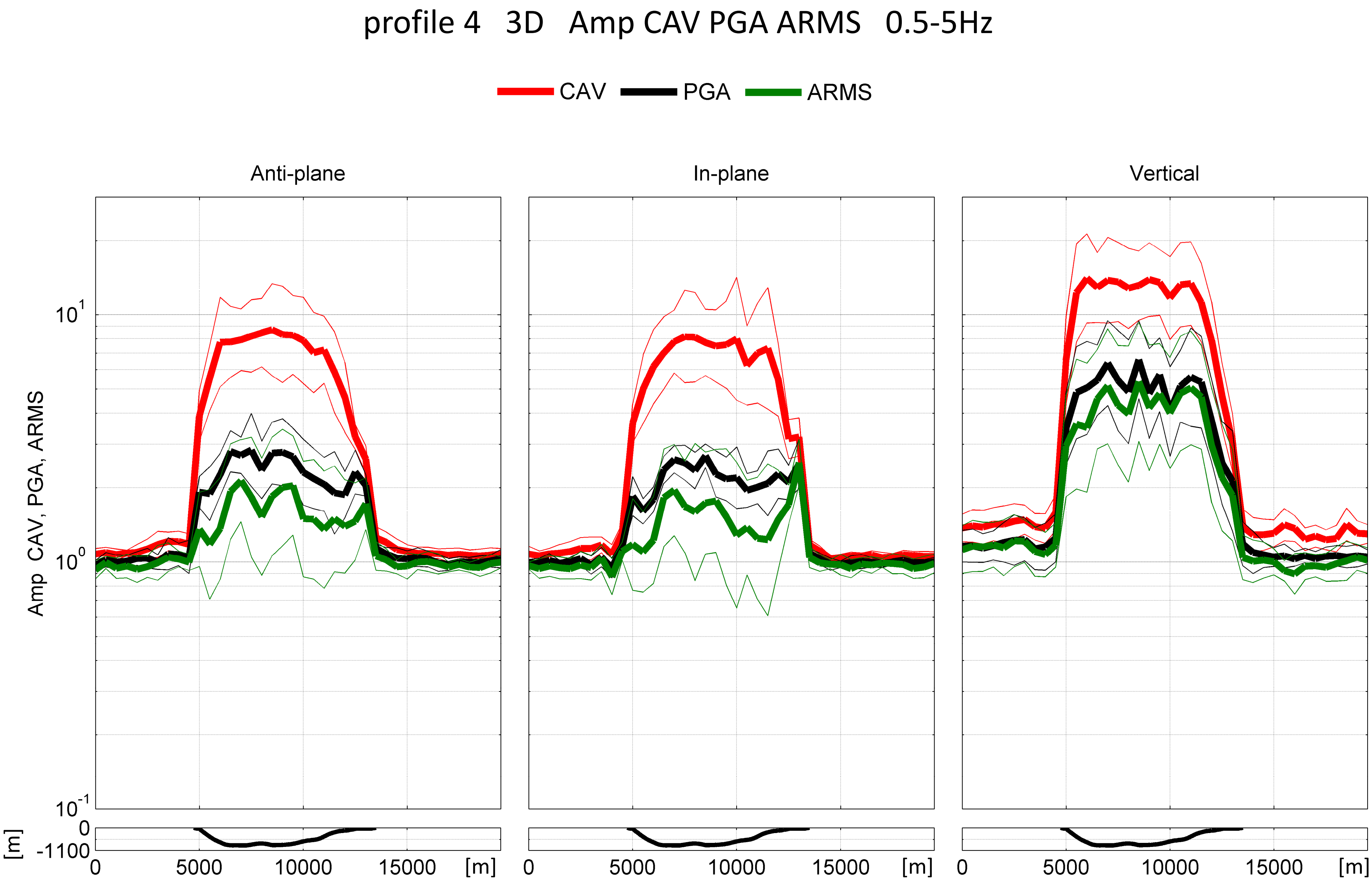

profile 4 3D Amp CAV PGA ARMS 0.5-5Hz
CAV
PGA
ARMS
Anti-plane
In-plane
Vertical
Amp CAV, PGA, ARMS
10^{1}
10^{0}
10^{-1}
[m]
0
-1100
0
5000
10000
15000
[m]

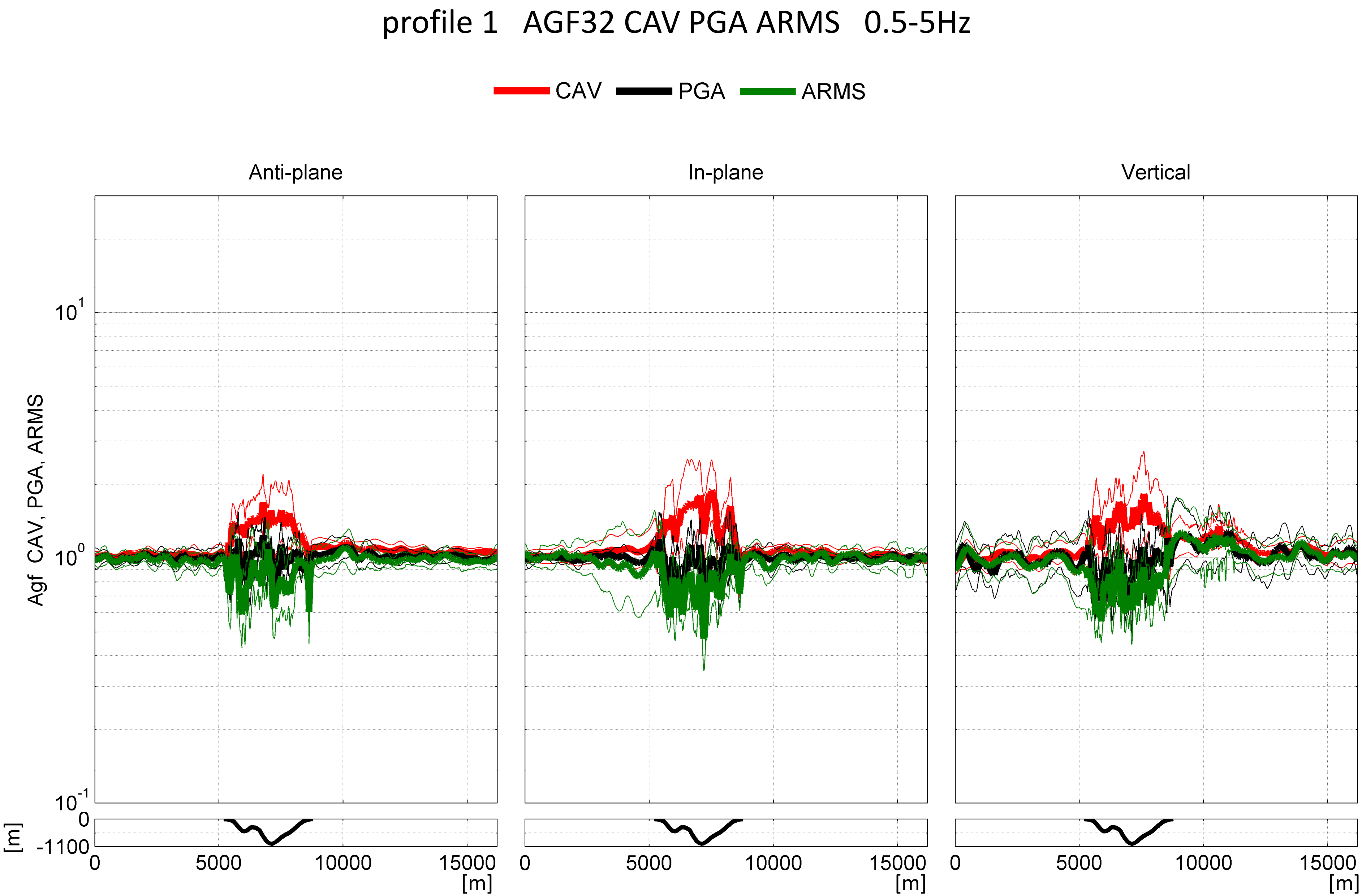

profile 1 AGF32 CAV PGA ARMS 0.5-5Hz
CAV
PGA
ARMS
Anti-plane
In-plane
Vertical
Agf CAV, PGA, ARMS
10^1
10^0
10^-1
[m]
0
-1100
0
5000
10000
15000
[m]

profile 4   AGF32 CAV PGA ARMS   0.5-5Hz

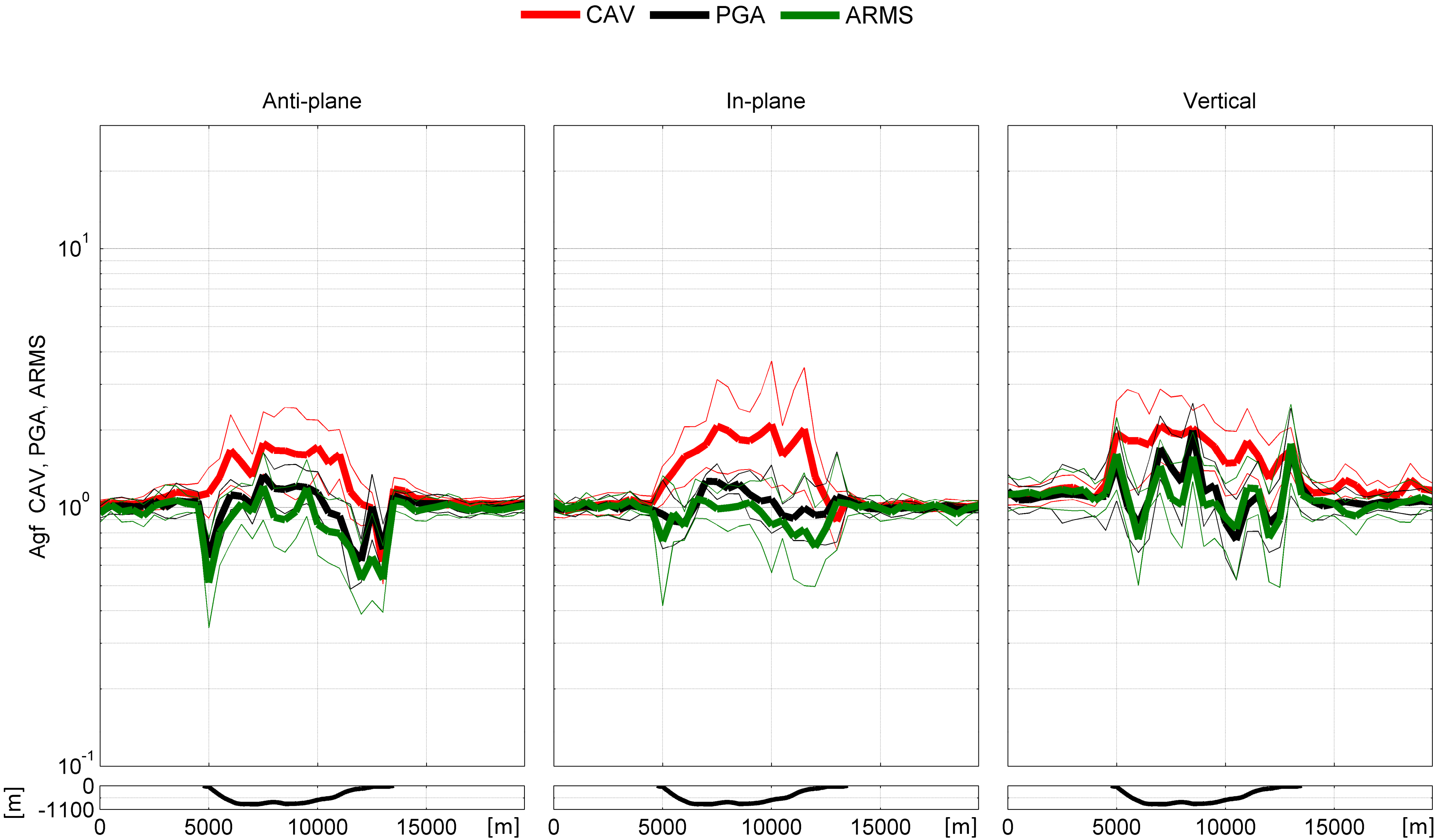

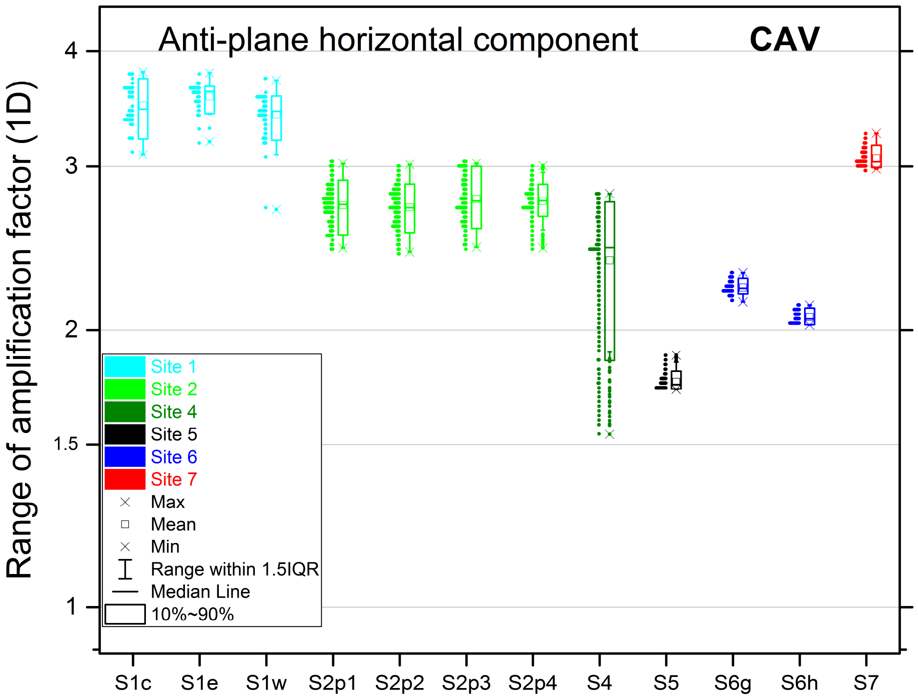
Anti-plane horizontal component
CAV
Range of amplification factor (1D)
4
3
2
1.5
1
Site 1
Site 2
Site 4
Site 5
Site 6
Site 7
Max
Mean
Min
Range within 1.5IQR
Median Line
10%~90%
S1c
S1e
S1w
S2p1
S2p2
S2p3
S2p4
S4
S5
S6g
S6h
S7

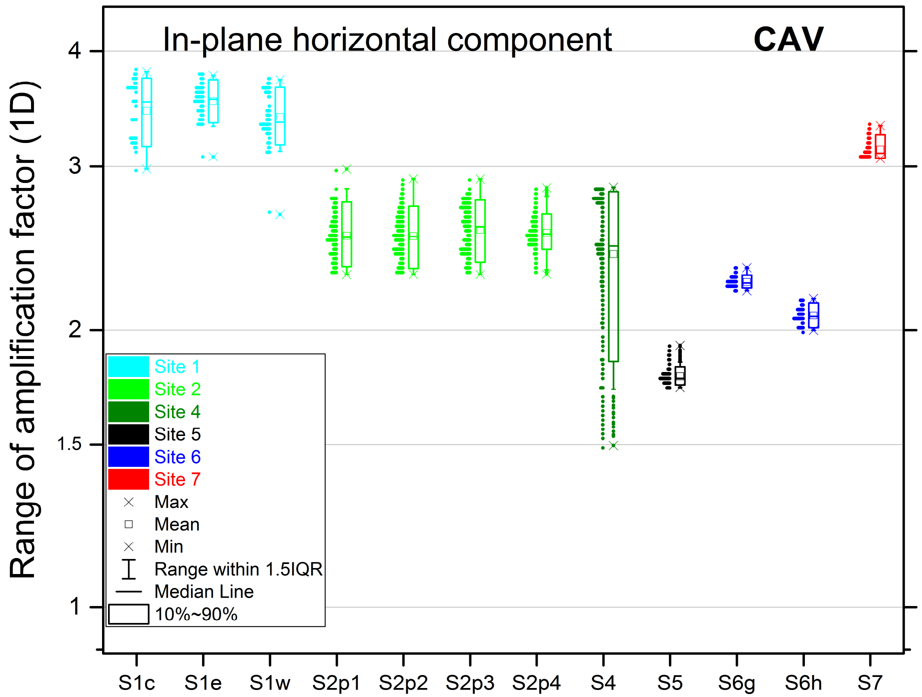
In-plane horizontal component
CAV
Range of amplification factor (1D)
4
3
2
1.5
1
Site 1
Site 2
Site 4
Site 5
Site 6
Site 7
Max
Mean
Min
Range within 1.5IQR
Median Line
10%~90%
S1c
S1e
S1w
S2p1
S2p2
S2p3
S2p4
S4
S5
S6g
S6h
S7

AF 1D
for CAV

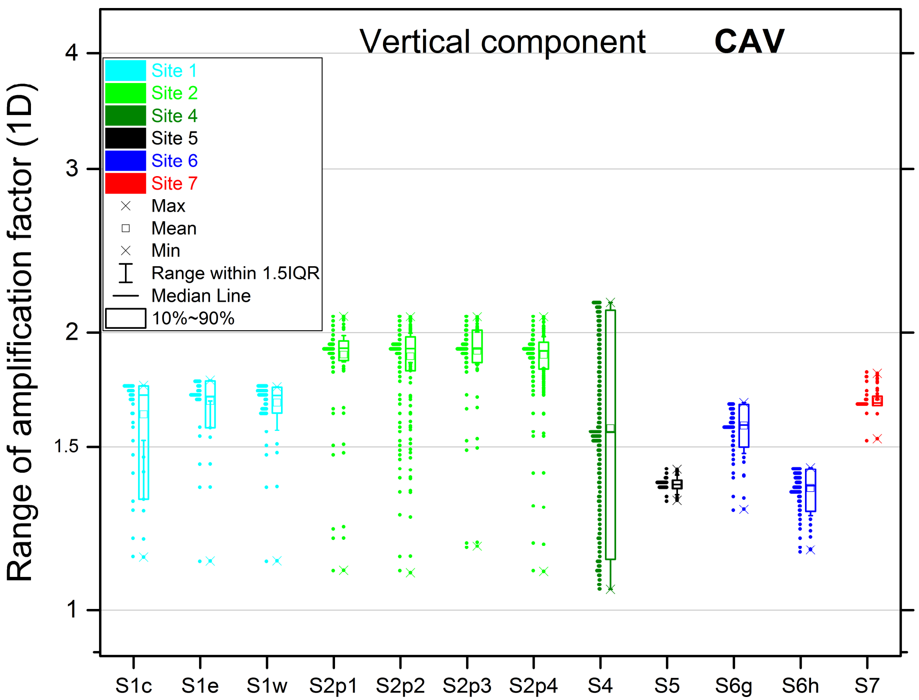
Vertical component
CAV
Range of amplification factor (1D)
4
3
2
1.5
1
Site 1
Site 2
Site 4
Site 5
Site 6
Site 7
Max
Mean
Min
Range within 1.5IQR
Median Line
10%~90%
S1c
S1e
S1w
S2p1
S2p2
S2p3
S2p4
S4
S5
S6g
S6h
S7

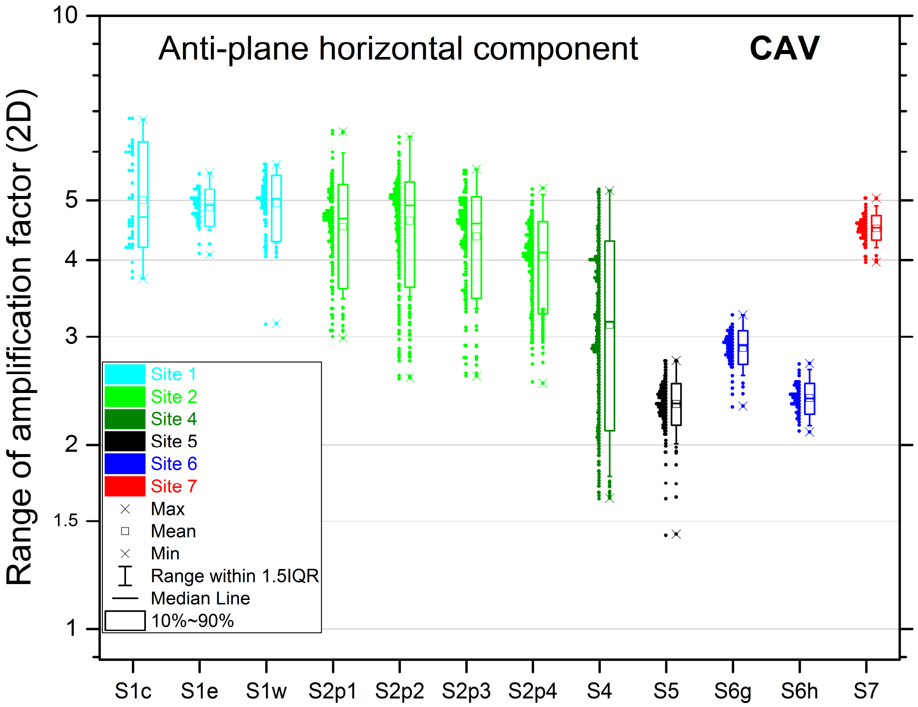
Anti-plane horizontal component
CAV
Range of amplification factor (2D)
10
5
4
3
2
1.5
1
Site 1
Site 2
Site 4
Site 5
Site 6
Site 7
Max
Mean
Min
Range within 1.5IQR
Median Line
10%~90%
S1c
S1e
S1w
S2p1
S2p2
S2p3
S2p4
S4
S5
S6g
S6h
S7

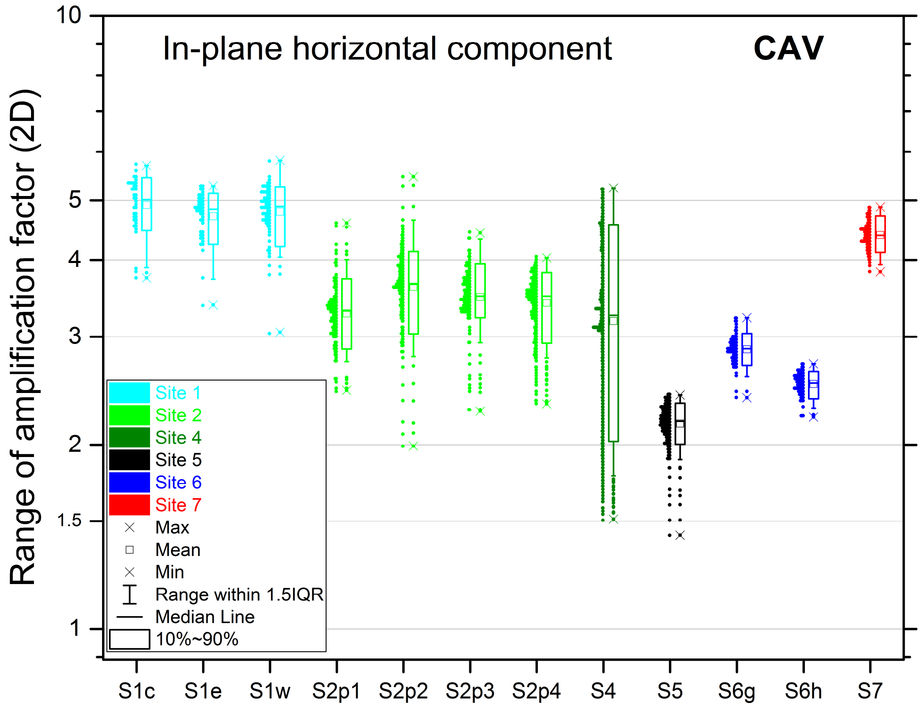
In-plane horizontal component
CAV
Range of amplification factor (2D)
10
5
4
3
2
1.5
1
Site 1
Site 2
Site 4
Site 5
Site 6
Site 7
Max
Mean
Min
Range within 1.5IQR
Median Line
10%~90%
S1c
S1e
S1w
S2p1
S2p2
S2p3
S2p4
S4
S5
S6g
S6h
S7

AF 2D
for CAV

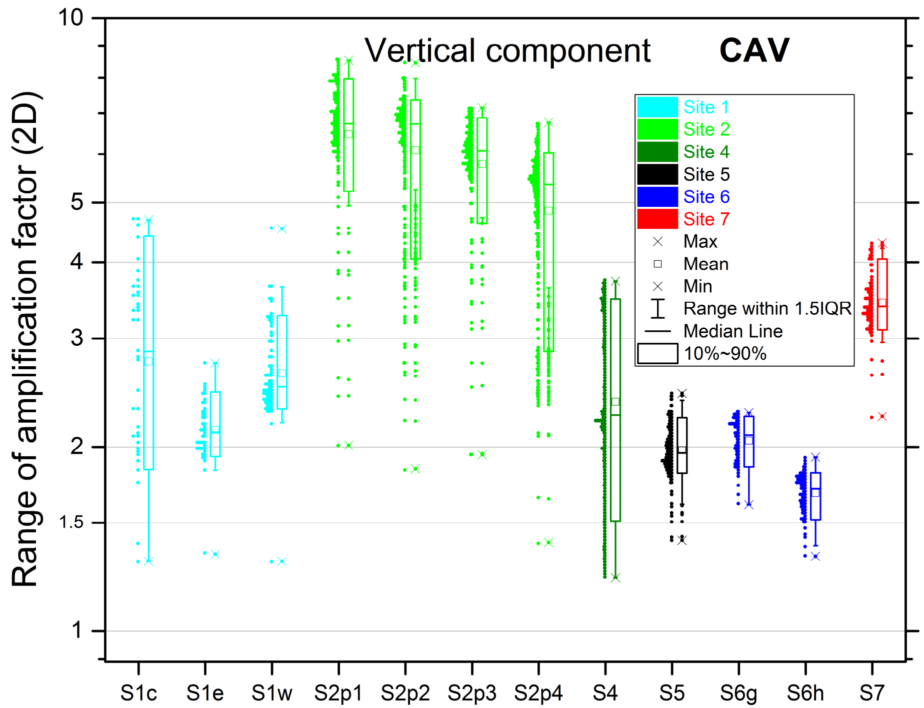
Vertical component
CAV
Range of amplification factor (2D)
10
5
4
3
2
1.5
1
Site 1
Site 2
Site 4
Site 5
Site 6
Site 7
Max
Mean
Min
Range within 1.5IQR
Median Line
10%~90%
S1c
S1e
S1w
S2p1
S2p2
S2p3
S2p4
S4
S5
S6g
S6h
S7

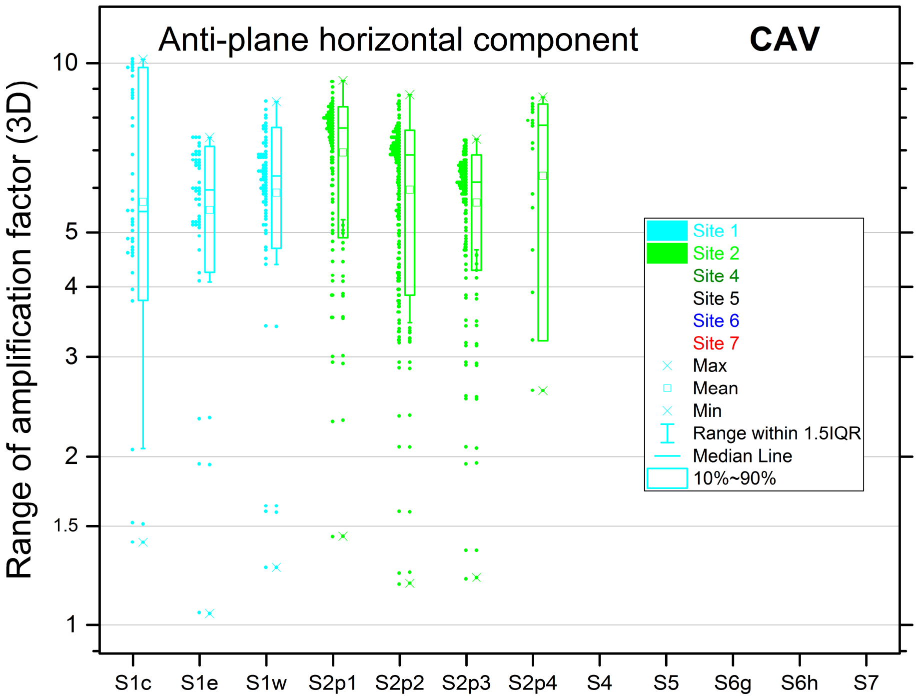
Anti-plane horizontal component
CAV
Range of amplification factor (3D)
10
5
4
3
2
1.5
1
S1c
S1e
S1w
S2p1
S2p2
S2p3
S2p4
S4
S5
S6g
S6h
S7
Site 1
Site 2
Site 4
Site 5
Site 6
Site 7
Max
Mean
Min
Range within 1.5IQR
Median Line
10%~90%

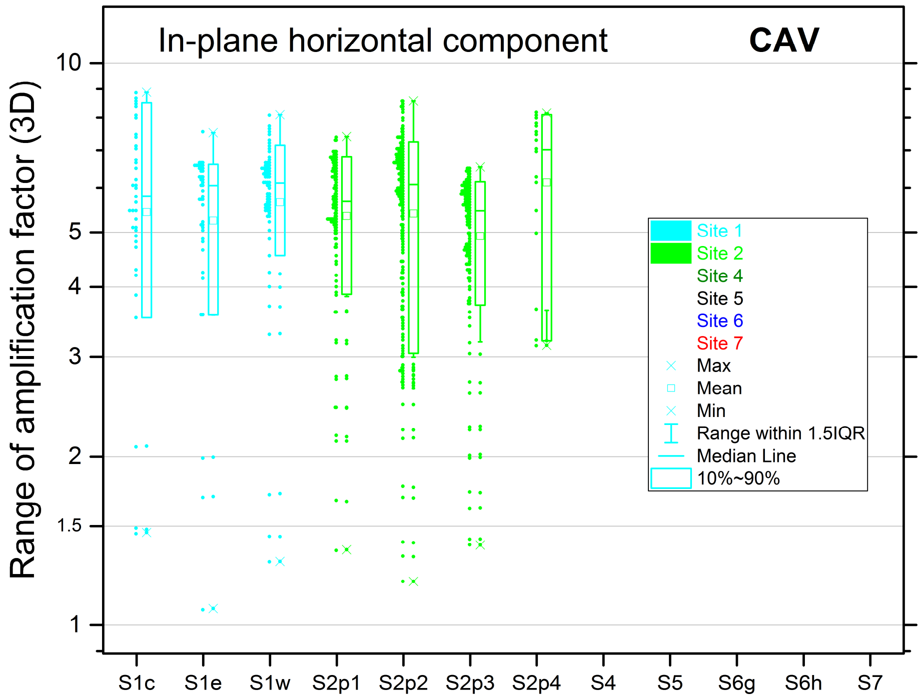
In-plane horizontal component
CAV
Range of amplification factor (3D)
10
5
4
3
2
1.5
1
S1c
S1e
S1w
S2p1
S2p2
S2p3
S2p4
S4
S5
S6g
S6h
S7
Site 1
Site 2
Site 4
Site 5
Site 6
Site 7
Max
Mean
Min
Range within 1.5IQR
Median Line
10%~90%

AF 3D
for CAV

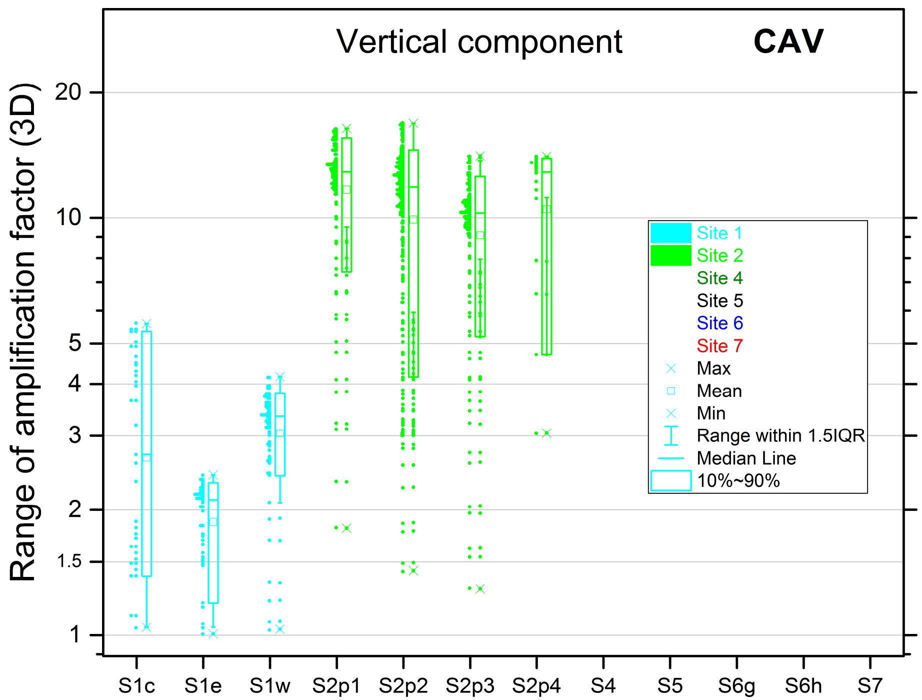
Vertical component
CAV
Range of amplification factor (3D)
20
10
5
4
3
2
1.5
1
S1c
S1e
S1w
S2p1
S2p2
S2p3
S2p4
S4
S5
S6g
S6h
S7
Site 1
Site 2
Site 4
Site 5
Site 6
Site 7
Max
Mean
Min
Range within 1.5IQR
Median Line
10%~90%

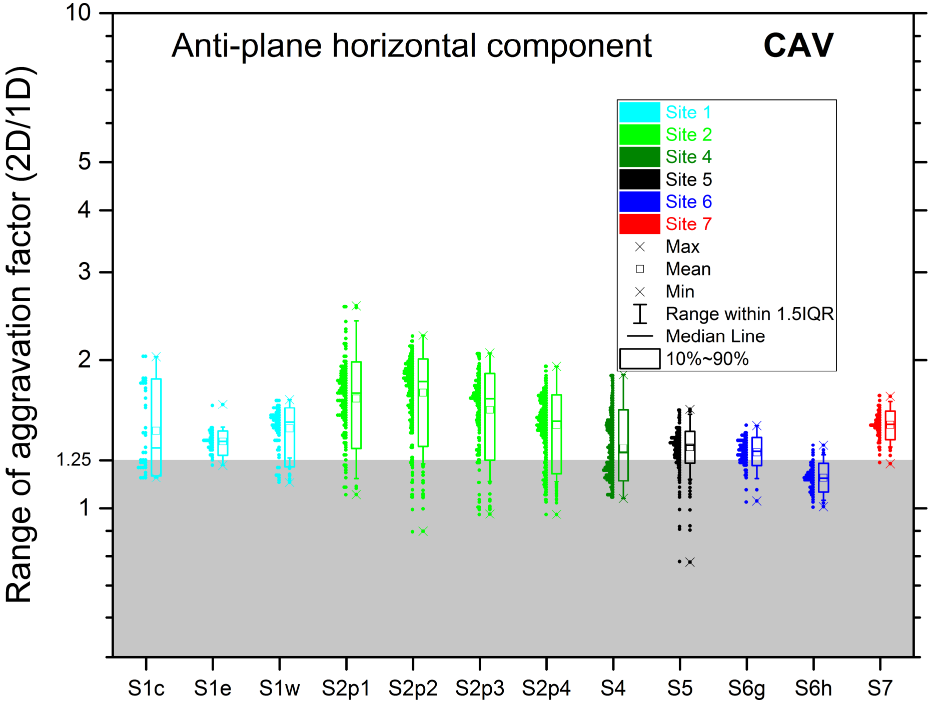

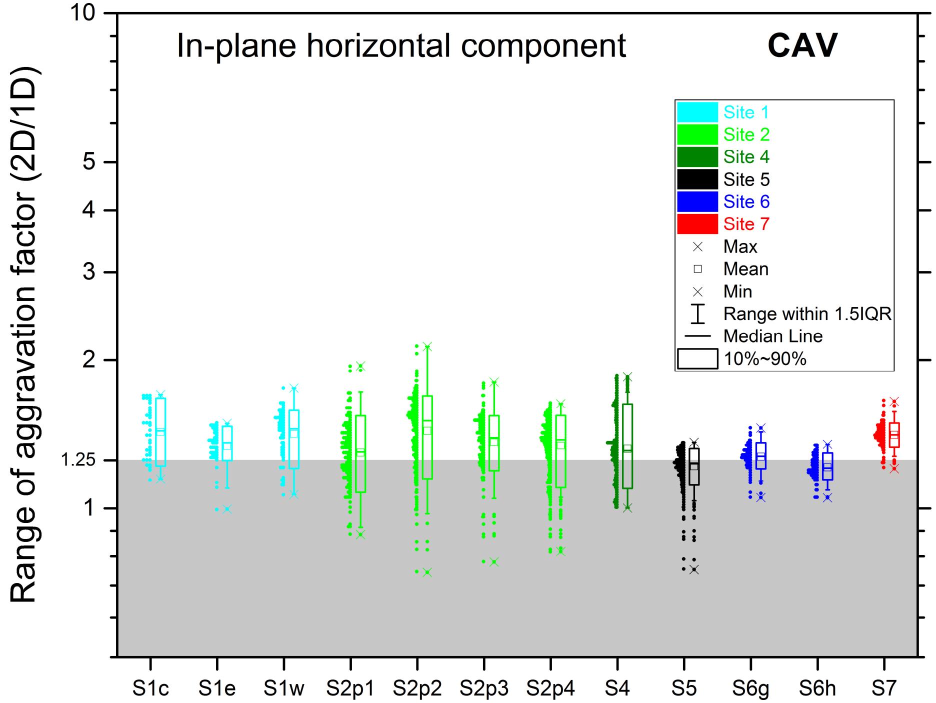

AGF 2D/1D
for CAV

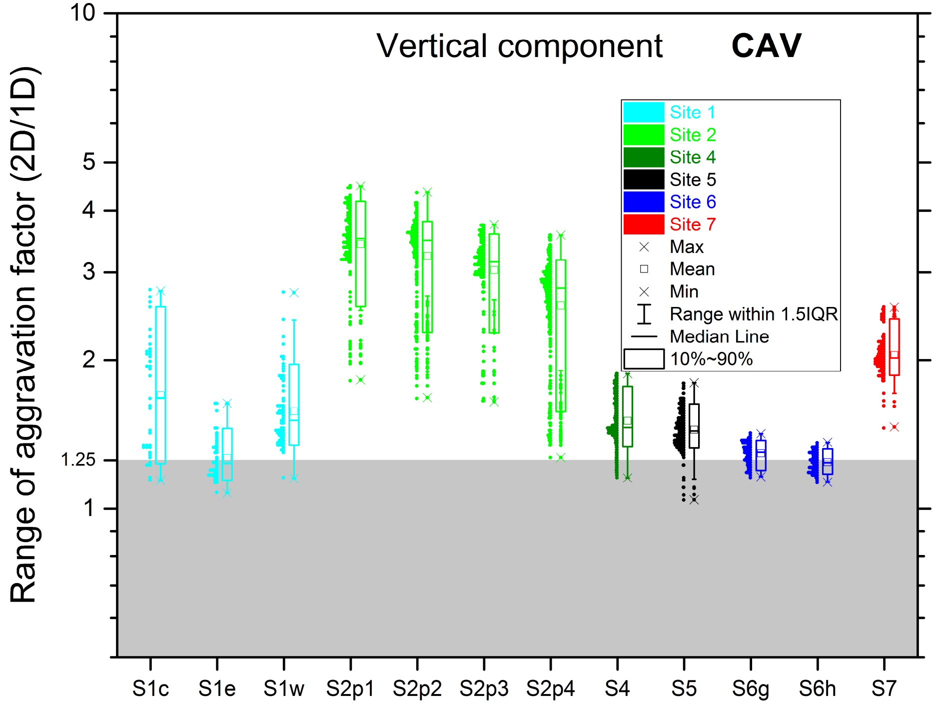

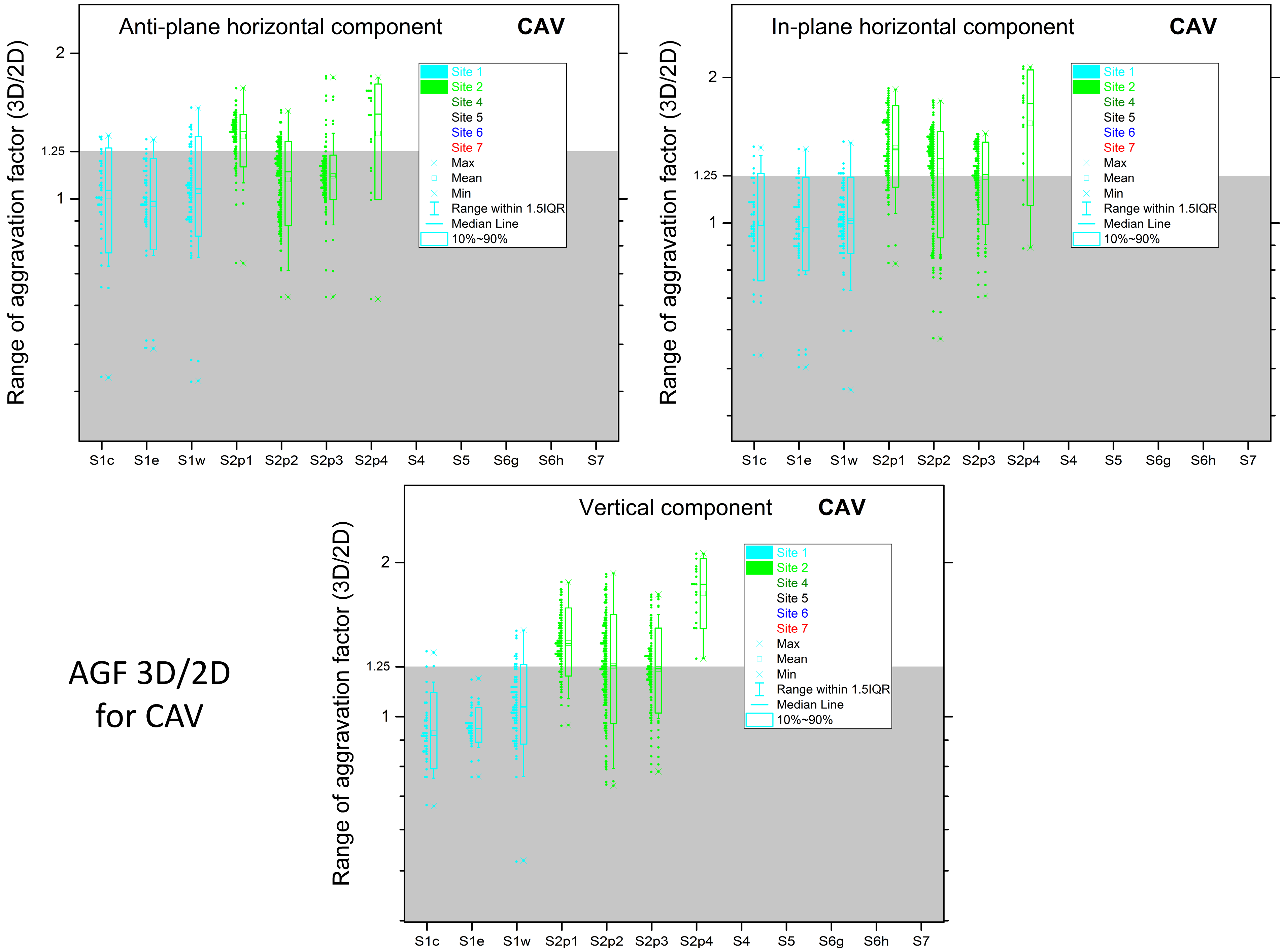

AGF 3D/2D
for CAV

we identified the following key structural parameters:

- overall geometry of the sediment-bedrock interface;
  detailed geometry close to margins of the basin or valley
  affects mainly motions close to the margins
- impedance contrast at the sediment-bedrock interface
- attenuation in sediments

conclusions

for all sites
there is at least one EGM characteristic
with significant 2D/1D aggravation factor

all characteristics exhibit significant 2D/1D aggravation factor
on the vertical component

the anti-plane and in-plane horizontal components
exhibit different behaviours

the CAV 2D/1D aggravation factor is significant
at all components and all sites;
1D simulations are not sufficient
for any of the investigated sites

3D effects are pronounced in the Grenoble valley (Site 2);
they are most visible on the CAV 3D/2D aggravation factors
(all components)

conclusions

the amplification factors and aggravation factors
(mainly for the vertical component)
increase with the impedance contrast;
this is mainly evident
at frequencies close to the fundamental resonant frequency

these conclusions are valid for all models

conclusions

the effect of attenuation
is more evident at higher frequencies

the amplification factor decreases with increasing attenuation;
this effect is more pronounced
with increasing local thickness of sediments

values of EGM characteristics are unrealistically large
if attenuation is neglected

the 2D/1D aggravation factor
is rather insensitive to variations in the attenuation;
the results suggest that
the effect of attenuation on the amplification
can be sufficiently estimated from 1D simulations

conclusions

the effect of the border slope variation
is not significant away from the border
(in terms of the evaluated EGM characteristics)

conclusions

the 2D/1D aggravation factors
are less sensitive to the simultaneous modifications of V_S and h
(with fixed resonant frequency)
than the amplification factors are

the least sensitivity is
at receivers atop thin sediments

the increase of the amplification factors
is due to the increase of the impedance contrast

conclusions

vertically incident plane waves
provide robust estimates of amplification factors
compared with point sources with specific azimuths

the plane-wave excitations should not, however,
replace a point DC source
if such a source better represents
a possible excitation from a known source zone

source variability induces
an additional variability in site response (± 10%)
which should be considered
when knowledge of location of potential seismic sources
is very poor

acknowledgement

This work has been done within the
SeIsmic Ground Motion Assessment (SIGMA) project.

The SIGMA project is funded and supported by
EDF, AREVA, CEA and ENEL.

thank you for the attention

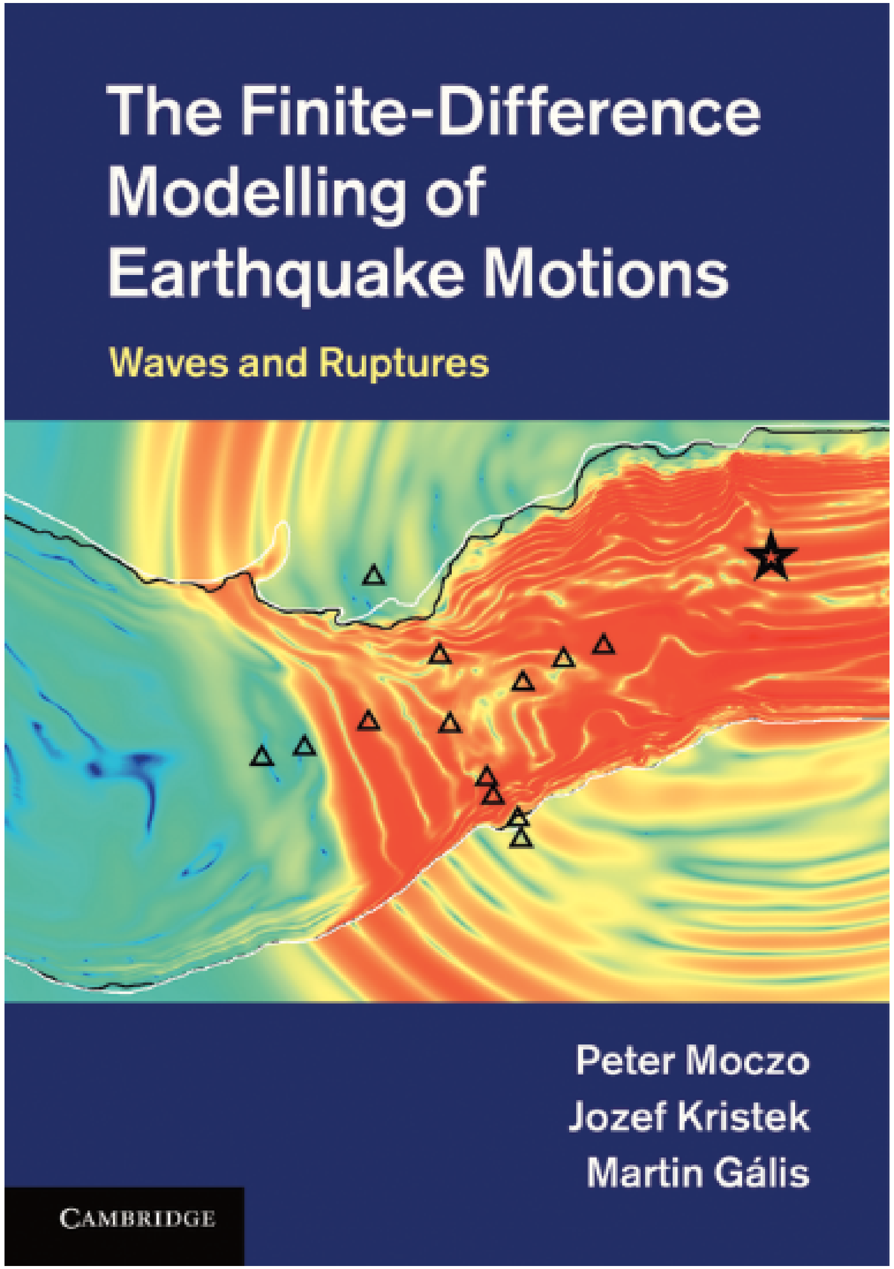
The Finite-Difference Modelling of Earthquake Motions
Waves and Ruptures
Peter Moczo
Jozef Kristek
Martin Gális
CAMBRIDGE